applied sciences

MDPI

Article

The Preparation and Characterization of Immobilized TiO_2/PEG by Using DSAT as a Support Binder

Wan Izhan Nawawi [1,*], Raihan Zaharudin [1,2], Mohd Azlan Mohd Ishak [1], Khudzir Ismail [2] and Ahmad Zuliahani [1]

[1] Faculty of Applied Sciences, Universiti Teknologi MARA, Perlis, 02600 Arau, Perlis, Malaysia; nurraihanzaharudin@gmail.com (R.Z.); azlanishak@perlis.uitm.edu.my (M.A.M.I.); zuliahani@perlis.uitm.edu.my (A.Z.)

[2] Faculty of Applied Sciences, Universiti Teknologi MARA, 40450 Shah Alam, Selangor, Malaysia; khudzir@salam.uitm.edu.my

* Correspondence: wi_nawawi@perlis.uitm.edu.my; Tel.: +60-4-9882-570; Fax: +60-4-9882-026

Academic Editor: Giorgio Biasiol
Received: 30 September 2016; Accepted: 13 December 2016; Published: 23 December 2016

Abstract: Immobilized TiO_2 was prepared by adding a small composition of polyethylene glycol (PEG) as a binder, and this paper reported for the very first time the formation of C=O from oxidized PEG, which acted as an electron injector in enhancing photoactivity. Water-based TiO_2 with PEG formulation was deposited by using a brush technique onto double-sided adhesive tape (DSAT) as a support binder to increase the adhesiveness of immobilized TiO_2. The photocatalytic activity of immobilized TiO_2-PEG was measured by photodegradation of 12 $mg \cdot L^{-1}$ methylene blue (MB) dye. The optimum condition of immobilized TiO_2-PEG was observed at TiO_2/PEG-2 (TP2) with 10:0.1 for the TiO_2/PEG ratio, which resulted in a 1.8-times higher photodegradation rate as compared to the suspension mode of pristine TiO_2. The high photodegradation rate was due to the formation of the active C=O bond from oxidized PEG binder in immobilized TiO_2-PEG as observed by Fourier transform infrared and X-ray photoelectron spectroscopy analyses. The presence of C=O has escalated the photoactivity by forming an electron injector to a conduction band of TiO_2 as proven by higher photoluminescence intensity obtained for TP2 as compared to pristine TiO_2. The TP2 sample has also increased its adhesiveness when DSAT is applied as a support binder where it can be recycled up to eight times and comparable to recent photocatalysis cycle developments.

Keywords: immobilization; titanium dioxide; oxidized PEG; support binder; methylene blue

1. Introduction

Titanium oxide (TiO_2) is a semiconductor that is widely known as a photocatalyst for the photodegradation of organic pollutants. According to Karimi et al. [1], when TiO_2 is illuminated by a light with energy higher than its band gap energy, electron–hole pairs diffuse out, creating negative electrons and oxygen that combine to become O_2^-, while the positive electric holes and water generate hydroxyl radicals. This highly active oxygen species can then oxidize organic pollutants. For over three decades, modifications on TiO_2 have improved two main issues. The first is to increase catalytic reaction performance where photocatalytic improvement of TiO_2 has been studied by many researchers. This is important in order to make the photocatalyst become active in the wide solar spectrum since the TiO_2 semiconductor is only active under high energy ultraviolet (UV) light [2]. Basically, there are two common types of modifications used in preparing the visible light TiO_2, which are the modification of bulk and the surface of TiO_2. Bulk modification often resulted in the narrowing of band gap energy, whereas surface modification does not change the band gap energy. However, surface modification successfully activates the photocatalyst under visible light by accepting

the electron from the sensitizing agent. The second is a recovery process of this photocatalyst after being treated with organic pollutants where the photodegradation of organic pollutants using TiO_2 is basically applied under suspension mode, which provides a high surface to volume ratio [3]. However, the recovery process of this suspension of TiO_2 powder with treated wastewater requires filtration. Separation of this nano-sized TiO_2 will clog the filter membrane and eventually penetrate through the porous filter, making the recovery process less effective [4]. Immobilization of TiO_2 has gained great interest since it can easily separate TiO_2 with treated wastewater [5]. Many papers with different types of polymers in immobilized TiO_2 have reported these findings after the first technique was discovered by Tennakone et al. [6]. Polymer is normally added as a binder in immobilized TiO_2 to improve its durability, temperature resisting ability and absorbance affinity towards pollutants [7–9], and some polymers are also able to increase TiO_2 photoactivity [10–25]. In most cases, prepared immobilized TiO_2 used solvent-based polymers, such as polythene sheets [10], thin polythene films [11], polystyrene (PS) beads [12], expanded polystyrene (EPS) beads [13], cellulose microspheres [14], fluoro polymer resins [15], polyethylene terephthalate (PET) bottles [16], polypropylene (PP) granules [17], cellulose fibers [18], polypropylene fabric (PPF) [19], polyvinyl chloride (PVC) [20], polycarbonate (PC), poly(methyl methacrylate) (PMMA) [21], polyvinyl acetate (PVAc) [22], poly(styrene)-co-poly(4-vinylpyridine) (PSP4VP) [23], rubber latex (an elastic hydrocarbon polymer) [24], parylene and tedlar [25].

Recently, water-based polymer binders have shown a vast potential of usage in immobilized TiO_2 for commercialization because they are environmentally friendly and economic. Water-based polymers, such as polyvinyl alcohol (PVA), polyaniline (PANI), polyvinyl pyrolydone (PVP) and polyethylene glycol (PEG), have performed greatly in water treatment separation, which also resulted in a significant photosensitivity to the visible light region [26–28]. For instance, Lei et al. [29] decorated TiO_2/PVA particles through a heat treatment method and obtained high photoactivity since the Ti–O–C bond generated led the immobilized sample to become fully in contact with the organic pollutant. TiO_2/PVA developed by Yang et al. [30] showed notable photoactivity under visible light irradiation due to the presence of conjugated polymer. They found that the conjugated molecules adsorbed on the TiO_2 surface and excited the electrons, thus injecting the electrons into the conduction band using visible light. PANI in immobilized TiO_2 studied by Nawi et al. [31] has shown a significant photocatalytic improvement by acting as a hole scavenger in TiO_2 under photodegradation of reactive red 4 (RR4) dye.

PEG is a polymer that is able to form a uniform surface, smooth coating and well-defined size particles [32]. PEG is a hydrophilic polymer, which is suitable for coating, as it reduces the formation of a cracked surface in the immobilized system [33]. Most of the reports on immobilized TiO_2 with PEG were identified to enhance photoactivity due to the effect of porosity and larger specific surface area [34,35]. Trapalis et al. [36] found that the porosity increased with PEG amount introduced in the film. However, no detailed study was conducted on surface chemical interaction between PEG and TiO_2 photocatalyst since the oxidation will only take place in the photocatalysis process. Technically, TiO_2 and polymer mixed ratios are a very critical factor. Excessive binder makes immobilized film strong, but reduces its photoactivity; however, a low amount of polymer makes TiO_2 leach out easily. This explained the lack of data discussed by other researchers on the surface chemical interaction of PEG in immobilized TiO_2. According to Wang et al. [37], visible light photocatalytic activity could also be enhanced by carbon-sensitized TiO_2, in which the carbon could be originated from titanium alkoxide and mainly existed as the C–C bonds (carbonaceous species), C=O and O=C–O bonds (carbonate species). Since visible light active TiO_2 using surface modification cannot be judged by using UV–Vis diffuse reflectance spectra (DRS), the easiest way to detect the characteristic of the visible light activity of this modified TiO_2 is through photoluminescence (PL) analysis where the highest PL intensity represented the highest photoactivity of the sample.

Previously, we have discovered the ability of double-sided adhesive tape (DSAT) to become a support binder in immobilized TiO_2-only [38]. DSAT has greatly improved immobilized TiO_2-only in

its strength and recyclability. Photocatalytic activity of this immobilized TiO_2-only, however, is slightly lower as compared to TiO_2 in suspension mode [39]. In this study, immobilized TiO_2 mixed with a small amount of PEG 6000 was prepared using DSAT as a support binder to observe the interaction between TiO_2 and PEG during photocatalysis process. The photoactivity of this immobilized TiO_2-PEG was observed by photodegradation of methylene blue, applied with specific parameters.

2. Results and Discussion

2.1. Characterization of Immobilized TiO_2

A method for immobilizing TiO_2 using DSAT was thoroughly described in the previous article [40]. In this work, a similar approach was taken where TiO_2 was coated onto DSAT as a support binder, but in the presence of a specific amount of PEG. Table 1 shows the experimental condition and pseudo first order rate constant of immobilized TiO_2 and the pristine TiO_2 sample in degrading methylene blue (MB) dye. As can be seen in Table 1, the increased amount of PEG in the formulation solutions has shown a significant increase of PEG in immobilized TiO_2-PEG samples detected by FTIR analysis. The 1160- and 2900-nm peaks of C–O and C–H stretching, respectively, as shown in Figure 1, corresponded to the PEG peaks based on similar peaks presented on the FTIR spectrum for pure PEG studied by Hyma et al. [41]. Photocatalytic activity of washed immobilized TiO_2-PEG was increased by increasing the amount of PEG from 0.05 to 0.1 g based on its photodegradation rate values. Photocatalytic activity starts to decrease beyond 0.1 g of PEG due to the agglomeration of PEG in TiO_2 particles, which makes it harder for a large amount of light to penetrate through the surface particles of TiO_2. Mukherjee et al. [39] have reported same behavior on immobilized TiO_2 with PVA. The catalyst loading effect of immobilized TiO_2 with 0.1 g of PEG samples has shown a different photocatalytic activity. Increasing the amount of catalyst loading from 0.05, 0.1, 0.2 and 0.3 grams will significantly increase the photodegradation rates from 0.039, 0.048, 0.048 and 0.087 min^{-1}, respectively. The high photodegradation rate at 0.3 g was due to the high adsorption capacity of the photocatalyst thin film composite that enhanced the decolorization process of MB dye, and eventually, this dye pollutant becomes degraded by the photocatalysis process. However, too much adsorption capacity beyond 0.3 g of catalyst loading for the immobilized TiO_2-PEG sample makes the photodegradation rate become 2.5-times slower. This observation was due to the excessive adsorbed MB dye on the surface of immobilized TiO_2-PEG, thus forming a thick layer coating on the TiO_2 surface and reducing the penetration of light for photocatalysis. It can be deduced that the immobilized TiO_2-PEG ratio of 10:0.1 at a 0.3-g catalyst loading is the optimum immobilized TiO_2-PEG with a photodegradation rate 1.8-times faster compared to pristine TiO_2; an optimum sample named as TiO_2/PEG-2 (TP2) (Table 1).

Table 1. The experimental condition and pseudo first order rate constant of immobilized TiO_2 and the control sample in degrading methylene blue (MB) dye.

TiO_2 Sample	Loading (g)	Mode (S [a] or I [b])	Amount of PEG (wt %)	Ratio (TiO_2/PEG)	S_{BET} ($m^2 \cdot g^{-1}$)	Rate Constant k (min^{-1})	
						Washed	Unwashed
Pristine TiO_2	0.3	S	0.00	10:0	50.00	0.048	-
TP0	0.3	I	0.00	10:0	49.25	0.054	0.048
TP1	0.3	I	0.05	10:0.05	-	0.080	0.041
TP2	0.3	I	0.10	10:0.1	88.30	0.087	0.017
TP3	0.3	I	0.15	10:0.15	-	0.081	0.024
TP4	0.3	I	0.20	10:0.2	-	0.040	0.030
TP5	0.05	I	0.10	10:0.1	-	0.039	0.039
TP6	0.1	I	0.10	10:0.1	-	0.048	0.048
TP7	0.2	I	0.10	10:0.1	-	0.048	0.028
TP8	0.4	I	0.10	10:0.1	-	0.030	0.015

[a] Suspension; [b] immobilize. S_{BET}: surface area; TP0 to TP8, TiO_2/PEG-0 to TiO_2-PEG-8.

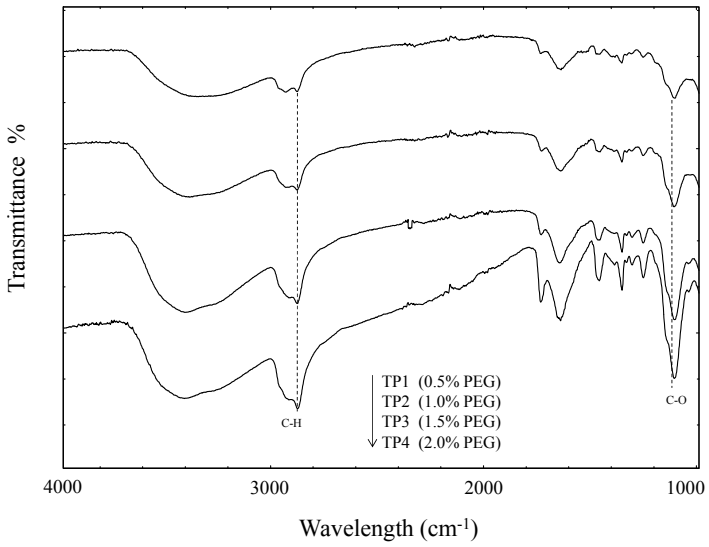

Figure 1. FTIR spectra of different percentages of polyethylene glycol (PEG) in immobilized TiO_2-PEG.

2.2. XRD Analysis

Figure 2 shows the XRD patterns for pristine TiO_2, TP0 (immobilized TiO_2 DSAT) and TP2 (immobilized TiO_2/PEG DSAT) samples. All peaks were detected as anatase and rutile phases. There is no phase transformation occurring in TP0 and TP2, since the immobilization processes of TP0 and TP2 were prepared under low temperature (120 °C). Phase transformation in the presence of organic binder was observed when the calcining temperature happened at 900 °C [42]. Wang et al. [43] also found that the phase transformation for TiO_2 calcined without organic binder occurred at a temperature of 700 °C onwards. All peaks for all samples correspond to the characteristic peak of the anatase and rutile phases of TiO_2 nanoparticles detected at 2θ from 15° to 65° by using low angle XRD. The XRD pattern in all samples shows different crystallinity as the sharp diffraction peaks displayed the good crystallinity of the prepared nanoparticles [44]. Pristine TiO_2 has the highest crystallinity as compared to TP0 and TP2, where TP2 is the lowest. This is due to the presence of DSAT and DSAT + PEG in TP0 and TP2, respectively. The increased porosity in both immobilized samples is the main factor for low crystallinity and broad peaks, as reported by Kim [45]. In short, no phase transformations occurred for any of the samples prepared under low heat temperature.

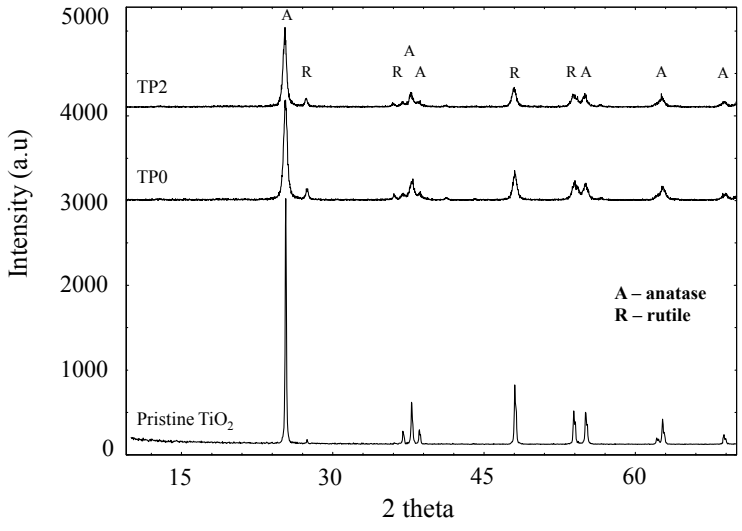

Figure 2. XRD patterns of pristine TiO_2, TP0 and TP2 samples.

2.3. SEM Images

Figure 3a,b shows the illustrative SEM images of the TP0 and TP2 surfaces after the photocatalytic degradation process. Few pores were observed in TP0, while for TP2, a variety of porous structures evolved on the surface. As shown in Figure 3b, the pore depth is larger around the PEG concentration of 8.0 g/100 mL as compared to TP0. It can be concluded that the porous structure of TP2 thin films is related to the molecular weight of PEG. The increased concentration of PEG has granted the formation of big pores. It is obvious that the catalyst morphologies shown in Figure 3b are highly presumed to perform an optimum photocatalytic activity. In this regard, Bing et al. [46] stated that the increased porosity in the immobilized TiO_2/PEG film is accountable for the increased photodegradation of the methyl orange model pollutant dye.

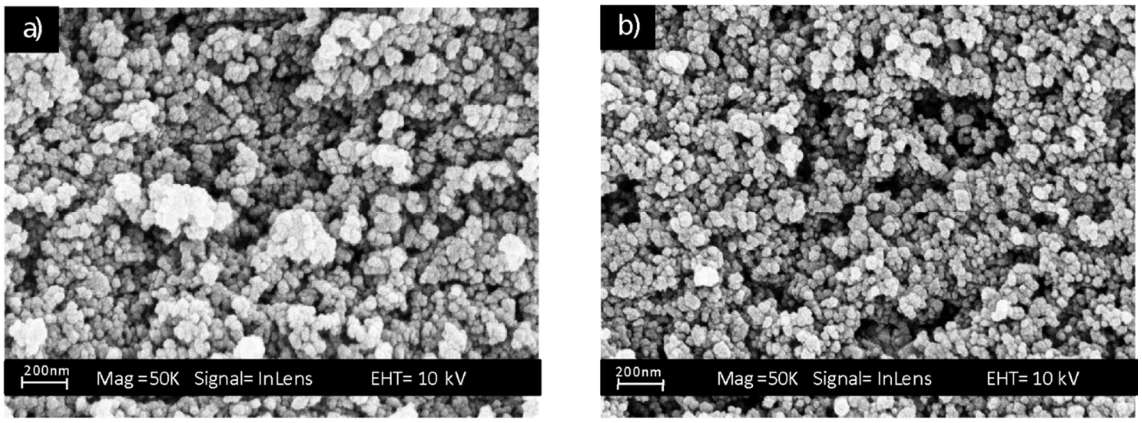

Figure 3. Scanning electron micrograph of surface morphologies for the (**a**) TP0 and (**b**) TP2 samples. EHT, extra high tension.

2.4. N_2 Adsorption-Desorption

The porous structure of TP2 is displayed by N_2 adsorption-desorption measurement as presented. It was found that the TP2 sample in Figure 4 exhibited the type IV nitrogen isotherm according to the International Union of Pure and Applied Chemists (IUPAC) classification; thus, this indicated that the TP2 sample is a mesoporous structure. According to Li et al. [47], a large surface area with a mesoporous structure is favorable to obtain a high photocatalytic activity, as it promotes adsorption, desorption and diffusion of reactants and products. The BET surface area of TP2 was enhanced to 88.3 $m^2 \cdot g^{-1}$ as compared to pristine TiO_2, which was circa 50 $m^2 \cdot g^{-1}$, where a 43.4% increment occurred due to the increased porosity and number of pores. By comparing TP0 with TP2, it is clear that the BET surface area for TP2 was increased up to 44% as compared to TP0, which was circa 49.25 $m^2 \cdot g^{-1}$. The results of TP2 surface area measurements are consistent with the results of photocatalytic activity where the TP2 sample gave a higher photocatalytic degradation rate of 0.087 min^{-1} as compared to pristine TiO_2, which is 0.048 and 0.054 min^{-1} for TP0, respectively. A higher BET surface area is vital for the adsorption and desorption of dyes and catalysts, since it encourages higher photocatalytic performance. In addition, PEG had successfully enhanced the possibility of the pollutant being trapped within the pores and showed better catalytic activity by providing additional surface active groups [48].

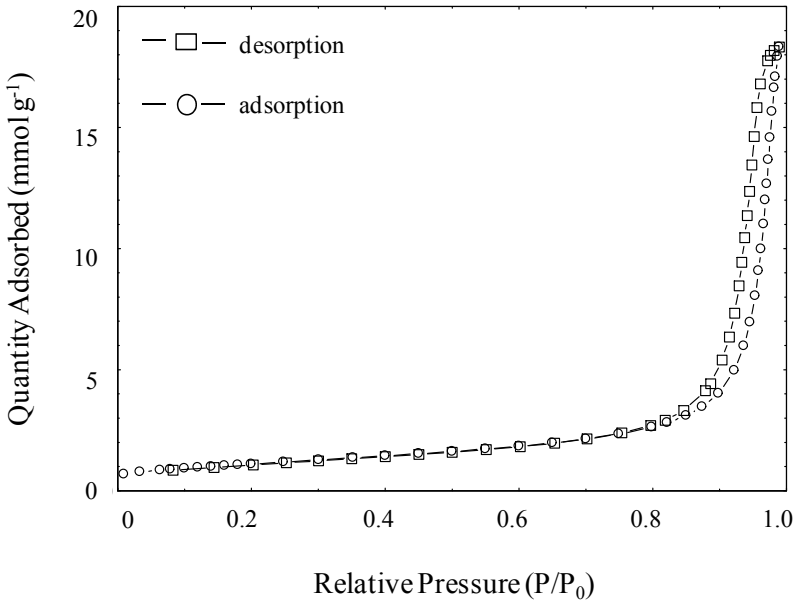

Figure 4. N_2 adsorption–desorption isotherms of the washed immobilized TiO_2/PEG (TP2).

2.5. FTIR

FTIR was used to acquire advanced information of the chemical bonding in TP0, washed TP2 and unwashed TP2 films, as shown in Figure 5. The spectra showed significant differences, which were due to the rising bands from the addition of PEG at 3389.77 and 3375.15 cm^{-1}. All spectra showed broad bands, which indicated the presence of O–H stretching vibrations of water absorbed with the hydroxyl group on the photocatalyst surface. The O–H bond was also noticed in both spectra at 1637.32 and 1637.45 cm^{-1}. The peak at 2900 cm^{-1} was detected in all spectra corresponding to C–H bonds.

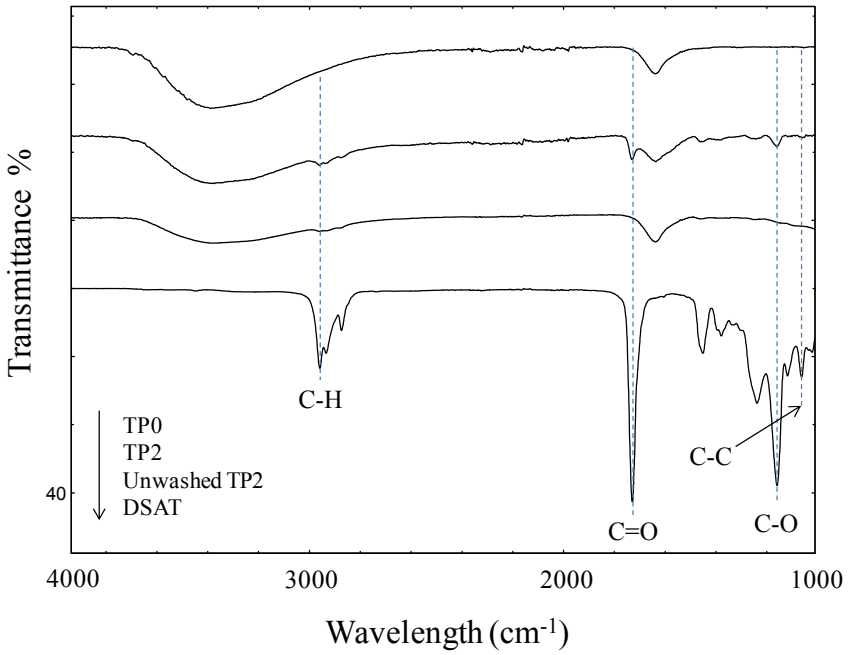

Figure 5. FTIR spectra of TP0, TP2 (washed TP2), unwashed TP2 and double-sided adhesive tape (DSAT) samples.

Interestingly, washed TP2 spectra showed a strong absorption in the region of 1705.02 cm^{-1}, which justified that the carbonate species C=O existed. On the other hand, a new peak detected at 1160.06 cm^{-1}, which is assigned to C–O species, was also present in the spectra. The presence of C=O affirmed that TiO_2 has reacted strongly with PEG, which could potentially lead to the high photoactivity of TP2. The C=O bonds detected were due to the oxidation of PEG in the irradiated TP2 film. As shown in Figure 5, the carbonaceous species C–C bond was detected in all samples except TP0. Generally, the IR spectrum for DSAT also produced the C=O bonds, but this factor can be discarded because during FTIR analysis of all samples, each sample's powder was carefully scratched and taken for analysis, excluding the DSAT. This is further supported by the IR spectrum of unwashed TP2, where the formation of C=O bonds was absent in Figure 5. In brief, even though the composition and structure of the investigated TP2 film do not greatly change, the photoactivity efficiency of TP2 in Table 1 was indirectly attributed to the formation of C=O bond that promotes more reactions to take place.

2.6. X-ray Photoelectron Spectroscopy (XPS)

XPS is used to determine the binding energy of elements detected in unwashed and washed immobilized TP2 samples in order to examine the effect of washing. This effect had successfully produced an oxidized PEG. The O1s and C1s spectra of TP2 unwashed are shown in Figure 6a,b, while Figure 6c,d represents the O1s and C1s spectra for washed TP2 sample.

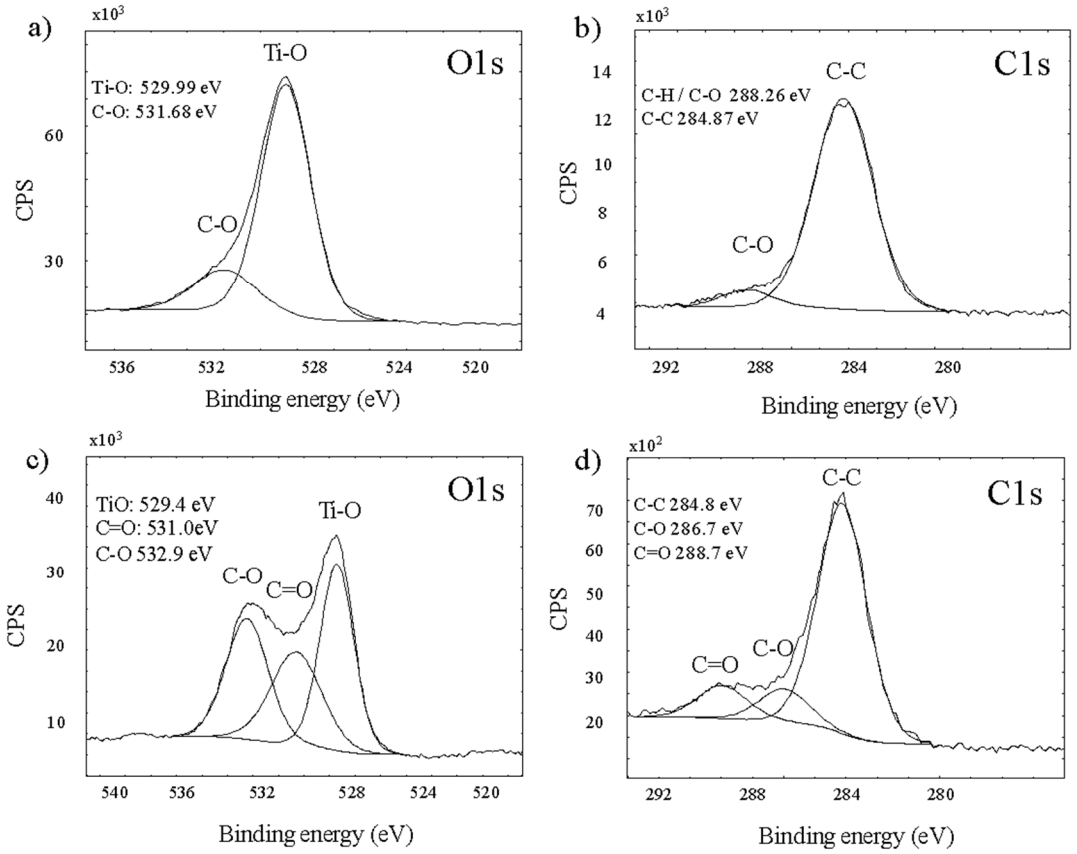

Figure 6. The O1s and C1s X-ray photoelectron spectroscopy (XPS) spectrums of immobilized for (**a**,**b**) unwashed TP2 and (**c**,**d**) washed TP2. CPS, cycles per second.

All samples demonstrated the chemical composition information where three elements existed: Ti, C and O. Figure 6a represents the O1s characteristic peaks of Ti–O and C–O at 529.9 and 531.6 eV, respectively, while C–O and C–C bonds are given by the values of 288.2 and 284.8 eV, respectively,

in Figure 6b. The O1s spectra in Figure 6c of washed TP2 revealed peaks at 529.4, 531.0 and 532.9 eV attributed to Ti–O, C–O and C=O bonds, respectively. Figure 6d shows the spectrum of washed TP2 in the C1s spectra deconvoluted into three distinct curves, which are represented by three forms of carbon as C–C, C–O and C=O at 284.8, 286.7 and 288.7 eV, respectively. As such, the formation of C=O bond can only be found in washed TP2. Yet, no peak for C=O bond was presented in unwashed TP2. This occurrence of C=O bond could be due to the oxidation process of hydroxyl radicals with PEG, introduced by the washed sample of TP2 in Figure 6c,d.

2.7. UV–Vis DRS and Visible Light Photodegradation Studies

UV–Vis diffuse reflectance spectra (UV–Vis DRS) of pristine TiO_2, unwashed and washed TP2 are shown in Figure 7a. All samples have a bit of difference in the pattern in UV–Vis diffuse reflectance spectra. It is obvious that pristine TiO_2 has the highest absorbance in UV–Vis spectra followed by washed TP2 and unwashed TP2 samples. Even though the modified TiO_2 or TP2 has lower absorbance as compared to unmodified pristine TiO_2, this result is expected because there are no bulk property modifications other than on the TP2 surface. Therefore, the chemical properties for TP2 and its band gap energy do not notably change even after surface alteration. According to Marcela et al. [49], from the solid state band theory, the absorption coefficient can be described as a function of incident photon energy; $(\alpha h\nu)^2 = A(h\nu - E_g)$, where α is the absorption coefficient (cm^{-1}), A is a constant, $h\nu$ (eV) is the energy of excitation and E_g is the band gap energy. The band gap energy can be performed by plotting $(\alpha h\nu)^2$ vs. $h\nu$. The Tauc plot on the photon energy-axis gives the value of the direct band gap energy of semiconductors [50].

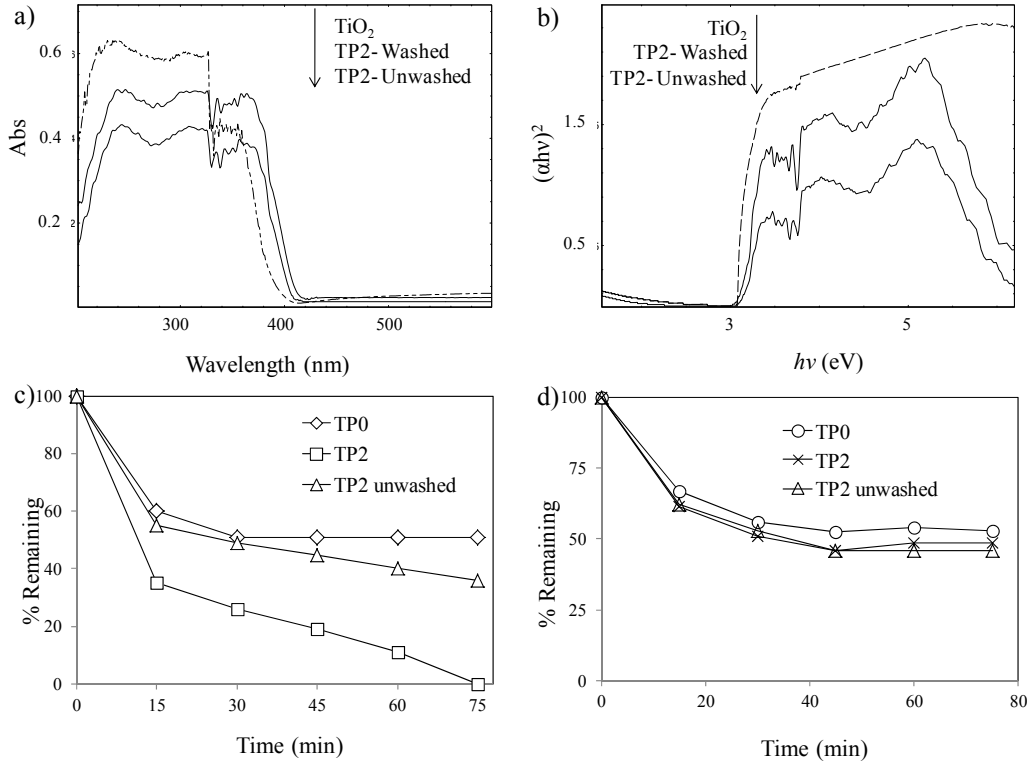

Figure 7. Graph plots for: (**a**) UV–Vis diffuse reflectance spectra (DRS); (**b**) Tauc's equation; (**c**) percentage remaining of MB dye under visible light irradiation; and (**d**) adsorption study. Abs, absorption.

Figure 7b shows a graph of $(\alpha h\nu)^2$ vs. $h\nu$, named as Tauc's graph plot. Theoretically, it seems that the band gap energy for all samples did not change and stayed approximately at 3.1 eV. As such,

the band gap energy of TiO_2 photocatalyst in TP0 did not change to a visible light active response, and this was similarly observed in Figure 7c where no photodegradation of 12 mg·L^{-1} MB was observed for TP0 under visible light irradiation. Only decolorization of MB was observed as reported on the adsorption site of the porous surface of TP0 as proven by the adsorption graph in Figure 7d and discussed in our previous study [51]. Unwashed TP2 showed a low photocatalytic degradation of MB dye due to the C–C bond in PEG that makes TP2 become slightly active under the visible light condition. Surprisingly, TP2 shows an active photodegradation under visible light where a complete decolorization of 12 mg·L^{-1} MB was achieved at 75 min. Although there is no shifting occur in band gap energy of TP2 due to its sole-surface modifications, it is believed that the visible light active ability in TP2 is due to the formation of C=O resulting from the oxidation of C–O bond in PEG detected by XPS and FTIR spectrums, which have been discussed earlier in Figures 5 and 6.

According to Wang et al. [37], C=O bond can act as an electron injector that initiated the formation of hydroxyl radical, thus eventually degraded the MB dye pollutant. TP2 had undergone the photoluminescence (PL) analysis at low activation energy irradiation to observe the effect of C=O activation under visible light irradiation. The PL emission spectra can be used to reveal the efficiency of charge carrier trapping, immigration and transfer and to understand the fate of photo-induced electrons and holes in a semiconductor [52,53]. It is known that the PL spectrum is the result of the recombination of excited electrons and holes where the lower PL intensity means a lower recombination rate of electron–hole pairs under light irradiation [54].

Figure 8 shows the PL spectra of pristine TiO_2, TP2 and unwashed samples of TP2 using the excitation wavelength of 500 nm. The photoluminescence spectrum in this study that was conducted under low excitation energy (500 nm) was meant to confirm that the excitation of electrons happened under a low energy level (visible light spectrum). It is shown that increased PL intensity leads to increased absorption of low excitation energy, resulting in higher photocatalytic activity [55]. It can be seen that all samples exhibited an obvious PL signal with a similarly-shaped curve at the wavelength range from 458 to 468 nm with the TP2 sample giving the highest PL intensity followed by TP0 and pristine TiO_2. However, the PL energy is smaller than the band gap energy of TiO_2. According to Jing et al., 2006 [56], they observed that some of the lower PL intensities of semiconductor materials are due to the presence of oxygen vacancy that acted as an electron scavenger, thus making electron recombination jump to the sub-band of TiO_2. Moreover, the energy at the 458 to 468-nm wavelength released from PL spectra is too high as compared to the excitation energy. This result is due to the presence of the sensitizer, which allowed for the absorption of low excitation energy to occur and formed an electron-hole pair. This electron is then subsequently jumped to the conduction band of TiO_2 and eventually recombined with the hole by releasing the high energy wavelength.

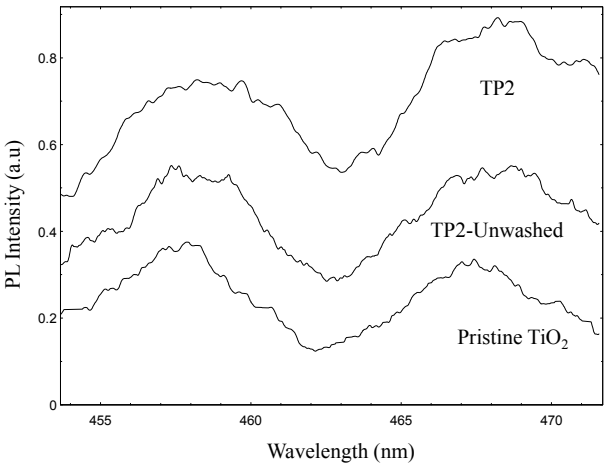

Figure 8. Photoluminescence spectra of pristine TiO_2, unwashed TP2 and washed TP2 samples. PL, photoluminescence.

As can be seen in Figure 8, all TP2 samples (washed and unwashed) have shown higher PL intensity as compared with pristine TiO_2. The intensity from the unwashed TP2 sample might be due to the presence of C–C bond that allowed for the electron to recombine under low excitation energy. The TP2 sample (washed) has recorded the highest PL intensity as compared to others. Based on the XPS and FTIR spectra, this TP2 sample has a C=O bond as an extra species where it is not found in pristine and unwashed TP2 samples. Hence, it can be concluded that the highest intensity of TP2 showed a significant presence of C=O bond, which acted as an electron injector in TP2 photocatalyst. The electrons that were injected to the conduction band of TiO_2 created a series of chain reactions, which help to achieve a complete 100% decolorization of 12 mg·L^{-1} MB dye at 75 min, as shown in Figure 7c.

2.8. Recyclability Study

For the stability study of the photocatalyst, the photocatalytic activity of TP2 was carried out by eight cycles of photodegradation of 12 mg·L^{-1} MB dye with 15-min intervals for 60 min in every cycle. Figure 9 shows the photodegradation cycle of MB dye using TP2. It was observed that each recycled application produced 100% removal of MB; indicating a sustainable photocatalytic efficiency characteristic. In other words, a strong interaction of TiO_2 with PEG occurred due to its strong chemisorption on the surface of TiO_2, where it was not easily leached out, even through up to eight times of repeated usage.

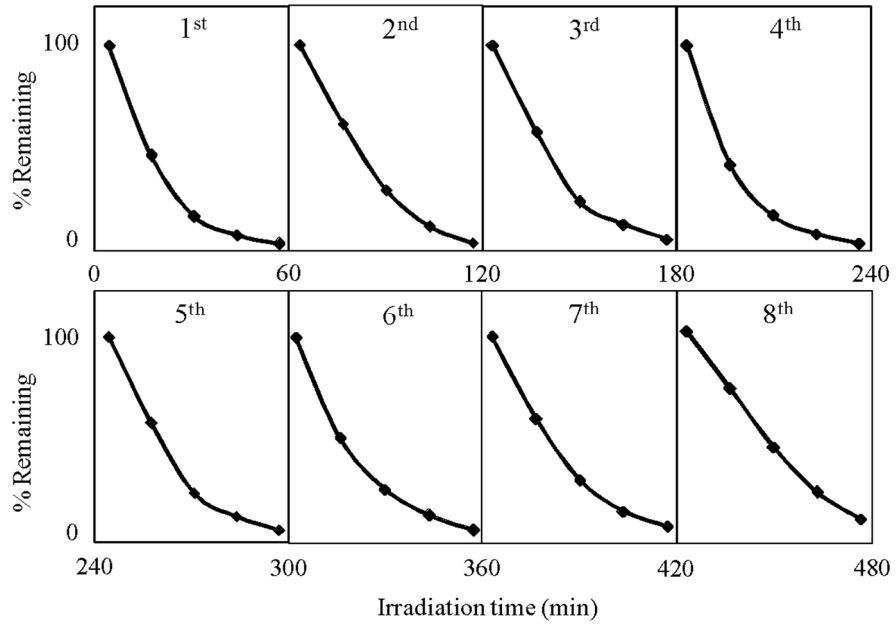

Figure 9. The recyclability graphs of TP2 under the photodegradation of MB dye.

2.9. Chemical Oxygen Demand Analysis

Decolorization of dye does not mean that there is complete removal of the organic carbons from the water samples. Mineralization, which is defined as the complete decomposition of organic compounds into CO_2 and H_2O, should be the target of any photocatalytic processes. One of the results of mineralization is the lowering of the chemical oxygen demand (COD) values of the treated samples. In this study, the presence of organic substances or intermediates can be detected by using a COD test. The COD test is attributed to the degradation of MB dye, as well as its by-products during the photocatalytic reaction using the TP2 sample. There is a possible contamination from DSAT, and these contaminations were completely cleaned up during the washing process prior to the photodegradation of MB dye. Figure 10 presents the detected COD values for the mineralization of MB dye versus

irradiation time. The COD values (mg·L^{-1}) detected were 0.81, 0.75, 0.60, 0.45, 0.30, 0.25, 0.10 and 0.05 and kept decreasing with time at 60, 120, 180, 240, 300, 360, 420 and 480 min, respectively. Hence, the complete mineralization of MB dye through the COD test was greatly caused by the improved diffusion of dye into photocatalyst layers, stemming from the porous surface of the TP2 photocatalyst sample.

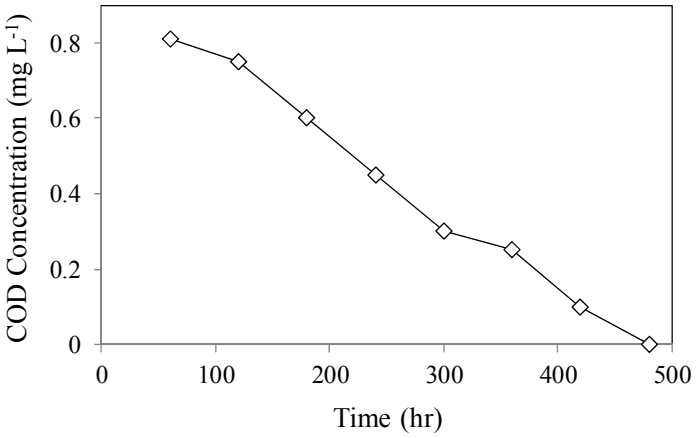

Figure 10. The chemical oxygen demand (COD) analysis of TP2 under photodegradation of MB dye.

3. Experimental Section

3.1. Preparation of Immobilized TiO_2-PEG

The sample solution was prepared by mixing 6.5 g of titanium dioxide (TiO_2) Degussa P25 powder (20% rutile, 80% anatase) in 50 mL distilled water added with 1 mL of 8% (*w/v*) of polyethylene glycol (Merck, Kenilworth, NJ, USA, MW = 6000). The sample solution was sonicated under an ultrasonic vibrator for 30 min to make it homogenized. The immobilized sample was prepared by using a brush-coating method applied onto a clean glass plate prior to taping with double-sided adhesive tape (DSAT). The wet TiO_2-PEG coated on glass was then dried using an 850-W hot blower with a temperature of about 120 °C until dry. The process was continued by repeating the process of coating onto dried TiO_2-PEG until the desired loading of immobilized TiO_2-PEG was achieved. Figure 11 shows the coated TiO_2 on DSAT attached to the glass plate with and without PEG binder.

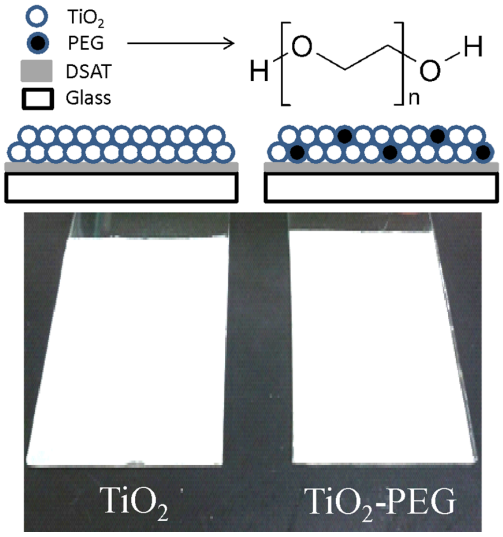

Figure 11. Picture of immobilized TiO_2 with and without PEG binder and the molecular structure of PEG.

3.2. Characterization Tests of Immobilized TiO_2/PEG DSAT

X-ray diffraction (XRD) spectra were obtained using a Rigakuminiflex II, X-ray diffractometer (Rigaku, Tokyo, Japan). Structural information of the films was obtained in the range of 2θ angles from 3° to 80° with a step size increment of 1.00 s/step. FTIR spectra of powder samples were recorded on Perkin Elmer Spectrum Version equipped with an attenuated total reflectance device (Perkin Elmer, Waltham, MA, USA) with a diamond crystal. Spectra were collected in a frequency range of 600 to 4000 cm^{-1} with 4 scans and a spectral resolution of 4 cm^{-1}. The morphology of the samples was observed with field-emitting scanning electron microscopy (FE-SEM, JSM-6700F, Akishima, Tokyo, Japan) with an accelerating voltage of 10 kV. The surface area of the immobilized TiO_2 film powders was measured by nitrogen adsorption using the BET equation at 77 K (Micrometrics ASAP 2020M + C, Norcross, GA, USA). A UV–Vis spectrophotometer UV-2550, Shimadzu was used to obtain the UV–Vis reflectance spectrum of the powder sample. X-ray photoelectron spectroscopy (XPS) with a Thermo ESCALAB 250 spectrometer using a radiation source of monochromatic Al Kα with the energy of 1486.6 eV, 200 W and a photoluminescence analyzer (JovinYvon, Chiyoda-ku, Tokyo, Japan) was used to determine the photoluminescence intensity of the samples.

3.3. Washing Process of Immobilized Samples

The washing process was conducted to oxidize PEG and also to clean all unwanted contaminants from immobilized TiO_2-PEG samples. The process was done by irradiating the immobilized samples in distilled water inside a glass cell of 150 mm × 10 mm × 80 mm (length × width × height). An aquarium pump model NS 7200 (Minjiang, Jiangmen, China) was used as an aeration source and irradiated with a 55-W fluorescent lamp for 1 h. The washing process was repeated once again by replacing the distilled water with a new amount of distilled water irradiated for another 30 min to affirm that zero contamination is achieved. This contamination was measured by using chemical oxygen demand analysis (COD) to detect any presence of organic compounds in washed distilled water. This process was done prior to the photodegradation of MB dye.

3.4. Photodegradation of MB Dye

The activity of the catalyst was tested by the degradation of methylene blue (MB), Fluka Analytical, with a chemical formula: $C_{12}H_{15}O_6$; and the molecular structure of MB is shown in Figure 12. The experimental procedure was the same method from our previous report [57]. The immobilized TiO_2-PEG was immersed into 20 mL of 12 $mg{\cdot}L^{-1}$ MB dye placed inside a glass cell under an aeration source. Light was then irradiated using a 55-W fluorescent lamp, Model Ecotone, with visible light intensity measured for about 461 and 6.7 $W{\cdot}m^{-2}$ of UV light detected as UV leakage. A 4-mL aliquot of treated MB dye was then taken out from the glass cell at 15-min intervals until it turned colorless by measuring its concentration using UV spectrophotometer Model HACH DR 1900 at a 661-nm λ max detector (Hach, Loveland, CO, USA). The experimental procedure was repeated by applying the same steps for different catalysts loading and different TiO_2/PEG ratios.

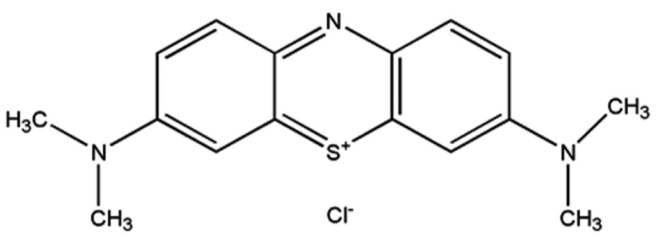

Figure 12. The molecular structure for methylene blue.

3.5. COD Analysis

Initially, the immobilized TiO_2/PEG DSAT (TP2) film was immersed in 20 mL of distilled water inside a glass cell under the irradiation of a 55-W compact fluorescent lamp. After 1 h of irradiation, the water sample was withdrawn and replaced with another set of distilled water using the same immobilized TiO_2/PEG film until 8 h of irradiation. The withdrawn water samples were then subjected to the COD test. It can be observed that MB dye and its generated by-products had undergone almost 100% complete mineralization after 8 h of irradiation using an immobilized TiO_2/PEG film.

3.6. Recyclability Study

The recyclability study was carried out to see the effect of immobilized TiO_2-PEG towards photodegradation stability. The experiment was conducted initially through the photodegradation method. Immobilized TiO_2-PEG was then subjected to the washing process using distilled water and irradiated for 30 min. Both the photodegradation and washing procedures for the immobilized the TiO_2-PEG sample were then repeated until eight cycles. The photodegradation percentage of MB in every cycle was recorded at every 15-min interval until MB became colorless.

4. Conclusions

An immobilized active TiO_2 photocatalyst was successfully prepared via adding a small amount of PEG as a binder onto a support binder of double-sided adhesive tape (DSAT). It was observed that utilization of 10:0.1 of a TiO_2/PEG ratio at 0.3 g of catalyst loading produced an immobilized TiO_2 with excellent photocatalytic activity. The preparation process did not produce any significant phase transformation, except for the typical TiO_2 phase. From the XPS and FTIR spectra, both observed that washed TiO_2-PEG (TP2) produced C=O bond that was confirmed to initiate the photocatalytic activity of the sample and to be 1.8-times higher than pristine TiO_2 under suspension mode in degrading 12 mg·L^{-1} MB dye. High PL intensity with low activation energy under immobilized TiO_2-PEG (TP2) proved that the presence of C=O increased the injected electron into the conduction band that eventually produced the hydroxyl radical agent used for the degradation of MB dye under visible light irradiation. Finally, TP2 or immobilized TiO_2-PEG was very stable and possessed excellent sustainable photocatalytic activity up to eight-times of reusability and comparable to recent photocatalysis cycles. As shown by the COD analysis, TP2 or immobilized TiO_2-PEG with DSAT leaves no organic pollutants during photodegradation cycles, which brings about a significant improvement in water quality.

Acknowledgments: We would like to thank the Ministry of Education (MOE), Malaysia, for providing generous financial support under the Research Acculturation Grant Scheme (RAGS) grants (600-RMI/RAGS 5/3 (35/2014)) in conducting this study and Universiti Teknologi MARA (UiTM) for providing all of the needed facilities.

Author Contributions: The experimental work and drafting of the manuscript were carried out by Raihan Zaharudin and assisted by Mohd Azlan Mohd Ishak, Khudzir Ismail and Ahmad Zuliahani participated in the interpretation of the scientific results and the preparation of the manuscript. Wan Izhan Nawawi supported the work and cooperation between UiTM Perlis and UiTM Shah Alam, supervised the experimental work, commented and approved the manuscript. The manuscript was written through comments and contributions of all authors. All authors have given approval to the final version of the manuscript.

Conflicts of Interest: The authors declare no conflict of interest.

References

1. Karimi, L.; Yazdanshenas, M.E.; Khajavi, R.; Rashidi, A.; Mirjalili, M. Optimizing the photocatalytic properties and the synergistic effects of graphene and nano titanium dioxide immobilized on cotton fabric. *Appl. Surf. Sci.* **2015**, *332*, 665–673. [CrossRef]
2. Hashimoto, K.; Irie, H.; Fujishima, A. TiO_2 photocatalysis: A historical overview and future prospects. *J. Appl. Phys.* **2005**, *44*, 8269. [CrossRef]
3. Pete, K.Y.; Sillanpää, M.M.; Onyango, M.S.; Aoyi, O. Kinetic modeling of the photocatalytic reduction of Cr(VI) in the presence of dye using composite photocatalyst. *J. Chem. Chem. Eng.* **2014**, *8*, 918–924.

4. McCullagh, C.; Robertson, J.M.; Bahnemann, D.W.; Robertson, P.K. The application of TiO_2 photocatalysis for disinfection of water contaminated with pathogenic micro-organisms: A review. *Res. Chem. Intermed.* **2007**, *33*, 359–375. [CrossRef]
5. Wang, T.; Wang, H.; Xu, P.; Zhao, X.; Liu, Y.; Chao, S. The effect of properties of semiconductor oxide thin films on photocatalytic decomposition of dyeing waste water. *Thin Solid Films* **1998**, *334*, 103–108. [CrossRef]
6. Tennakone, K.; Tilakaratne, C.T.K.; Kottegoda, I.R.M. Photocatalytic degradation of organic contaminants in water with TiO_2 supported on polythene films. *J. Photochem. Photobiol. A* **1995**, *87*, 177–179. [CrossRef]
7. Tasić, N.; Branković, Z.; Marinković-Stanojević, Z.; Branković, G. Effect of binder molecular weight on morphology of TiO_2 films prepared by tape casting and their photovoltaic performance. *Sci. Sinter.* **2012**, *44*, 365–372. [CrossRef]
8. Mukherjee, D. Development of a novel TiO_2 polymeric photocatalyst for water purification both under UV and solar illuminations. Ph.D. Thesis, The University of Western Ontario, London, ON, Canada, 2011.
9. Suzana, Š.; Lidija, Ć.; Ljubas, D.; Svetličić, V.; Houra, I.F.; Tomašić, N. Photocatalytic degradation of Lissamine Green B dye by using nanostructured sol–gel TiO_2 films. *J. Alloys Compd.* **2011**, *37*, 1153–1160.
10. Naskar, S.; Pillay, S.A.; Chanda, M. Photocatalytic degradation of organic dyes in aqueous solution with TiO_2 nanoparticles immobilized on foamed polyethylene sheet. *J. Photochem. Photobiol. A* **1998**, *113*, 257–264. [CrossRef]
11. Dhananjeyan, M.R.; Mielczarski, E.; Thampi, K.R.; Buffat, P.; Bensimon, M.; Kulik, A.; Kiwi, J. Photodynamics and surface characterization of TiO_2 and Fe_2O_3 photocatalysts immobilized on modified polyethylene films. *J. Phys. Chem. B* **2001**, *105*, 12046–12055. [CrossRef]
12. Fabiyi, M.E.; Skelton, R.L. Photocatalytic mineralisation of methylene blue using buoyant TiO_2-coated polystyrene beads. *J. Photochem. Photobiol. A* **2000**, *132*, 121–128. [CrossRef]
13. Magalhaes, F.; Lago, R.M. Floating photocatalysts based on TiO_2 grafted on expanded polystyrene beads for the solar degradation of dyes. *Sol. Energy* **2009**, *83*, 1521–1526. [CrossRef]
14. Nagaoka, S.; Hamasaki, Y.; Ishihara, S.I.; Nagata, M.; Iio, K.; Nagasawa, C.; Ihara, H. Preparation of carbon/TiO_2 microsphere composites from cellulose/TiO_2 microsphere composites and their evaluation. *J. Mol. Catal. A* **2002**, *177*, 255–263. [CrossRef]
15. Sopyan, I.; Watanabe, M.; Murasawa, S.; Hashimoto, K.; Fujishima, A. A film-type photocatalyst incorporating highly active TiO_2 powder and fluororesin binder: Photocatalytic activity and long-term stability. *J. Electroanal. Chem.* **1996**, *415*, 183–186. [CrossRef]
16. Fostier, A.; Pereira, H.; Rath, M.D.S.S.; Guimarães, S. Arsenic removal from water employing heterogeneous photocatalysis with TiO_2 immobilized in PET bottles. *Chemosphere* **2008**, *72*, 319–324. [CrossRef] [PubMed]
17. Meng, X.; Wang, H.; Qian, Z.; Gao, X.; Yi, Q.; Zhang, S.; Yang, M. Preparation of photodegradable polypropylene/clay composites based on nanoscaled TiO_2 immobilized organoclay. *Polym. Compos.* **2009**, *30*, 543–549. [CrossRef]
18. Mounir, B.; Pons, M.N.; Zahraa, O.; Yaacoubi, A.; Benhammou, A. Discoloration of a red cationic dye by supported TiO_2 photocatalysis. *J. Hazard Mater.* **2007**, *148*, 513–520. [CrossRef] [PubMed]
19. Han, H.; Bai, R. Highly effective buoyant photocatalyst prepared with a novel layered-TiO_2 configuration on polypropylene fabric and the degradation performance for methyl orange dye under UV–Vis and Vis lights. *Sep. Purif. Technol.* **2010**, *73*, 142–150. [CrossRef]
20. Nawi, M.A.; Ngoh, S.Y.; Zain, S.M. Photoetching of immobilized TiO_2-ENR_{50}-PVC composite for improved photocatalytic activity. *Int. J. Photoenergy* **2012**, *2012*, 859294. [CrossRef]
21. Zeng, J.; Liu, S.; Cai, J.; Zhang, L. TiO_2 immobilized in cellulose matrix for photocatalytic degradation of phenol under weak UV light irradiation. *J. Phys. Chem. C* **2010**, *114*, 7806–7811. [CrossRef]
22. Kim, C.; Kim, J.T.; Kim, K.S.; Jeong, S.; Kim, H.Y.; Han, Y.S. Immobilization of TiO_2 on an ITO substrate to facilitate the photoelectrochemical degradation of an organic dye pollutant. *Electrochim. Acta* **2009**, *54*, 5715–5720. [CrossRef]
23. Murugan, E.; Rangasamy, R.; Jebaranjitham, J.N. Immobilization of TiO_2 and TiO_2 [Au] nanoparticles onto the poly (4-vinylpyridine) matrix and their photocatalysis. *Adv. Sci. Lett.* **2012**, *6*, 250–256. [CrossRef]
24. Sriwong, C.; Wongnawa, S.; Patarapaiboolchai, O. Photocatalytic activity of rubber sheet impregnated with TiO_2 particles and its recyclability. *Catal. Commun.* **2008**, *9*, 213–218. [CrossRef]

25. Zhi, Y.; Keppner, H.; Laub, D.; Mielczarski, E.; Mielczarski, J.; Kiwi-Minsker, L. Photocatalytic discoloration of methyl orange on innovative parylene–TiO_2 flexible thin films under simulated sunlight. *Appl. Catal. B* **2008**, *79*, 63–71.
26. Gu, L.; Wang, J.; Qi, R.; Wang, X.; Xu, P.; Han, X. A novel incorporating style of polyaniline/TiO_2 composites as effective visible photocatalysts. *J. Mol. Catal. A* **2012**, *357*, 19–25. [CrossRef]
27. Song, Y.; Zhang, J.; Yang, H.; Xu, S.; Jiang, L.; Dan, Y. Preparation and visible light-induced photo-catalytic activity of H-PVA/ TiO_2 composite loaded on glass via sol–gel method. *Appl. Surf. Sci.* **2014**, *292*, 978–985. [CrossRef]
28. Moreno, C.; Preda, J.M.; Predoana, S.; Zaharescu, L.; Anastasescu, M.; Nicolescu, M.; Mihaila, M.M. Effect of polyethylene glycol on porous transparent TiO_2 films prepared by sol–gel method. *Ceram. Int.* **2014**, *40*, 2209–2220. [CrossRef]
29. Lei, P.; Wang, F.; Gao, X.; Ding, Y.; Zhang, S.; Zhao, J.; Liu, S.; Yang, M. Immobilization of TiO_2 nanoparticles in polymeric substrates by chemical bonding for multi-cycle photodegradation of organic pollutants. *J. Hazard Mater.* **2012**, *227*, 185–194. [CrossRef] [PubMed]
30. Yang, H.; Zhang, J.; Song, Y.; Xu, S.; Jiang, L.; Dan, Y. Visible light photocatalytic activity of C-PVA/TiO_2 composites for degrading rhodamine B. *Appl. Surf. Sci.* **2015**, *324*, 645–651. [CrossRef]
31. Razak, S.; Nawi, M.A.; Haitham, K. Fabrication, characterization and application of a reusable immobilized TiO_2–PANI photocatalyst plate for the removal of reactive red 4 dye. *Appl. Surf. Sci.* **2014**, *319*, 90–98. [CrossRef]
32. Zainab, M.; Jeefferie, A.R.; Masrom, A.K.; Rosli, Z.M. Effect of PEG molecular weight on the TiO_2 particle structure and TiO_2 thin films properties. *Adv. Mater. Res.* **2012**, *364*, 76–80. [CrossRef]
33. Santos, Á.A.; Acevedo-Peña, P.; Córdoba, E.M. Enhanced photocatalytic activity of TiO_2 films by modification with polyethylene glycol. *Quim. Nova* **2012**, *35*, 1931–1935. [CrossRef]
34. Wang, S.H.; Wang, K.H.; Dai, Y.M.; Jehng, J.M. Water effect on the surface morphology of TiO_2 thin film modified by polyethylene glycol. *Appl. Surf. Sci.* **2013**, *264*, 470–475. [CrossRef]
35. Chang, H.; Jo, E.H.; Jang, H.D.; Kim, T.O. Synthesis of PEG-modified TiO_2–$InVO_4$ nanoparticles via combustion method and photocatalytic degradation of methylene blue. *Mater. Lett.* **2013**, *92*, 202–205. [CrossRef]
36. Trapalis, C.; Keivanidis, C.P.; Kordas, G.; Zaharescu, M.; Crisan, M.; Szatvanyi, A.; Gartner, M. TiO_2 (Fe^{3+}) nanostructured thin films with antibacterial properties. *Thin Solid Films* **2003**, *431*, 186–190. [CrossRef]
37. Wang, P.; Zhou, T.; Wang, R.; Lim, T.T. Carbon-sensitized and nitrogen-doped TiO_2 for photocatalytic degradation of sulfanilamide under visible-light irradiation. *Water Res.* **2011**, *45*, 5015–5026. [CrossRef] [PubMed]
38. Ismail, W.I.N.W.; Ain, S.K.; Zaharudin, R. New TiO_2/DSAT immobilization system for photodegradation of anionic and cationic dyes. *Int. J. Photoenergy* **2015**, *2015*, 232741. [CrossRef]
39. Mukherjee, D.; Barghi, S.; Ray, A.K. Preparation and charaterization of the TiO_2 immobilized polymeric photocatalyst for degradation of aspirin under UV and solar light. *Processes* **2013**, *2*, 12–23. [CrossRef]
40. Zaharudin, R.; Ain, S.K.; Bakar, F.; Azami, M.S.; Nawawi, W.I. A comparison study of new TiO_2/PEG immobilized techniques under normal and visible light irradiation. *MATEC Web Conf.* **2016**, *47*, 05017. [CrossRef]
41. Hyma, P.; Abbulu, K. Formulation and characterisation of self-microemulsifying drug delivery system of pioglitazone. *Biomed. Prev. Nutr.* **2013**, *3*, 345–350. [CrossRef]
42. Zhang, M.; An, T.; Hu, X.; Wang, C.; Sheng, G.; Fu, J. Preparation of visible light-driven g-C_3N_4@ZnO hybrid photocatalyst via mechanochemistry. *Appl. Catal. A* **2014**, *260*, 215–222. [CrossRef]
43. Wang, C.C.; Lee, C.K.; Lyu, M.D.; Juang, L.C. Photocatalytic degradation of C.I. Basic Violet 10 using TiO_2 catalysts supported by Y zeolite: An investigation of the effects of operational parameters. *Dyes Pigment.* **2008**, *76*, 817–824. [CrossRef]
44. Rafiee-Pour, H.A.; Hamadanian, M.; Koushali, S.K. Nanocrystalline TiO_2 films containing sulfur and gold: Synthesis, characterization and application to immobilize and direct electrochemistry of cytochrome c. *Appl. Surf. Sci.* **2016**, *363*, 604–612. [CrossRef]
45. Kim, D.S.; Kwak, S.Y. The hydrothermal synthesis of mesoporous TiO_2 with high crystallinity, thermal stability, large surface area, and enhanced photocatalytic activity. *Appl. Catal. A* **2007**, *323*, 110–118. [CrossRef]

46. Guo, B.; Liu, Z.; Hong, L.; Jiang, H. Sol gel derived photocatalytic porous TiO_2 thin films. *Surf. Coat. Technol.* **2005**, *198*, 24–29. [CrossRef]
47. Li, B.; Huang, H.; Guo, Y.; Zhang, Y. Diatomite-immobilized BiOI hybrid photocatalyst: Facile deposition synthesis and enhanced photocatalytic activity. *Appl. Surf. Sci.* **2015**, *353*, 1179–1185. [CrossRef]
48. Tiwari, D.; Lalhriatpuia, C.; Lee, S.M.; Kong, S.H. Efficient application of nano-TiO_2 thin films in the photocatalytic removal of Alizarin Yellow from aqueous solutions. *Appl. Surf. Sci.* **2015**, *353*, 275–283. [CrossRef]
49. Rosu, C.M.; Suciu, C.R.; Dreve, S.V.; Danut, T.; Bratu, I.; Indrea, E. The influence of PEG/PPG and of the annealing temperature on TiO_2-based layers properties. *Rev. Roum. Chim.* **2012**, *57*, 15–21.
50. Franz, S.; Perego, D.; Marchese, O.; Lucotti, A.; Bestetti, M. Photoactive TiO_2 coatings obtained by plasma electrolytic oxidation in refrigerated electrolytes. *Appl. Surf. Sci.* **2016**, *385*, 498–505. [CrossRef]
51. Ain, S.K.; Azami, M.S.; Zaharudin, R.; Bakar, F.; Nawawi, W.I. Photocatalytic study of new immobilized TiO_2 technique towards degradation of reactive red 4 dye. *MATEC Web of Conf.* **2016**, *47*, 05019. [CrossRef]
52. Yu, C.; Jimmy, C.Y.; Fan, C.; Wen, H.; Hu, S. Synthesis and characterization of Pt/BiOI nanoplate catalyst with enhanced activity under visible light irradiation. *Mater. Sci. Eng.* **2010**, *166*, 213–219. [CrossRef]
53. Li, B.F.; Li, X.Z. The enhancement of photodegradation efficiency using Pt–TiO_2 catalyst. *Chemosphere* **2002**, *48*, 1103–1111. [CrossRef]
54. Li, B.F.; Li, X.Z. Photocatalytic properties of gold/gold ion-modified titanium dioxide for wastewater treatment. *Appl. Catal. A* **2002**, *228*, 15–27. [CrossRef]
55. Teixeira, S.; Martins, P.M.; Lanceros-Méndez, S.; Kühn, K.; Cuniberti, G. Reusability of photocatalytic TiO_2 and ZnO nanoparticles immobilized in poly(vinylidene difluoride)-*co*-trifluoroethylene. *Appl. Surf. Sci.* **2016**, *384*, 497–504. [CrossRef]
56. Jing, L.; Xin, B.; Yuan, F.; Xue, L.; Wang, B.; Fu, H. Effects of surface oxygen vacancies on photophysical and photochemical processes of Zn-doped TiO_2 nanoparticles and their relationships. *J. Phys. Chem. B* **2006**, *110*, 17860–17865. [CrossRef] [PubMed]
57. Nawawi, W.I.; Ain, S.K.; Zaharudin, R.; Sahid, S. Multi-cycle photodegradation of anionic and cationic dyes by new TiO_2/DSAT immobilization system. *Appl. Mech. Mater.* **2016**, *835*, 353–358. [CrossRef]